

Giant magnetoresistance of copper/permalloy multilayers

P. Holody, W. C. Chiang,* R. Loloee, J. Bass, W. P. Pratt, Jr., and P. A. Schroeder

Department of Physics and Astronomy and Center for Fundamental Materials Research, Michigan State University, East Lansing, Michigan 48823-1116

(Received 31 March 1998; revised manuscript received 23 July 1998)

Current perpendicular (CPP) and current in-plane (CIP) magnetoresistances (MR) have been measured on sputtered Cu/Py (Py=Permalloy) multilayers at 4.2 K. The CPP-MR is several times larger than the CIP-MR. For fixed Py layer thickness, $t_{\text{Py}}=1.5$ nm, both the CPP and CIP MR's show oscillations with increasing t_{Cu} with a period similar to that previously reported for the CIP-MR. The CPP data for Cu thicknesses large enough that exchange interactions between Py layers are small are analyzed using the two spin-current model for both infinite and finite spin-diffusion length in Py. The very low coercive field of Py leads to a larger than usual uncertainty in the derived parameters, because of the uncertainty in the degree of antiparallel alignment required for the analysis. Three alternative analyses give bulk and interface spin-dependent anisotropy parameters, β , and γ , of comparable size, so that both must be considered in determining the CPP-MR. Our preferred values, based upon an assumed $l_{\text{sf}}^{\text{Py}}=5.5\pm 1$ nm, are $\beta=0.65\pm 0.1$ and $\gamma=0.76\pm 0.1$. These values produce good fits to the CPP-MR's of Co/Cu/Py/Cu multilayers.

[S0163-1829(98)01442-8]

I. INTRODUCTION

Giant magnetoresistance (GMR) in multilayers composed of alternating ferromagnetic (F) and nonmagnetic (N) layers is of great interest both scientifically and technologically. GMR is the reduction in resistance, often large, when an applied magnetic field H aligns the magnetizations M_i of the F layers parallel (P) to each other. The largest GMR is expected to occur when interactions between the F layers cause the M_i of adjacent layers to align antiparallel (AP) to each other in the initial zero-field state. Theoretical analysis of GMR focuses upon the change in resistance R , $\Delta R=R(\text{AP})-R(\text{P})$, that occurs when the alignment changes from AP to P. We formally define the MR as

$$\text{MR}=\Delta R/R(\text{P}). \quad (1)$$

Experimentally, $R(\text{P})$ is easily obtained by raising H above the saturation field, H_s , of the multilayer. Estimating $R(\text{AP})$ is more difficult, and is one of the main issues that we address.

The low coercive field ($H_c\sim$ a few Oe) of Permalloy ($\text{Ni}_{100-x}\text{Fe}_x$ with $x\sim 20=\text{Py}$) makes the MR of multilayers containing it of technological interest. We will see that this same low H_c complicates the determination of $R(\text{AP})$ for Cu/Py multilayers, because the low-field magnetic state of the system can easily be perturbed by stray H fields during growth.

The current in plane CIP-MR of Cu/Py multilayers was measured by Parkin¹ and later by others.² The present paper contains extensive data and analysis for Cu/Py with current flow perpendicular to the plane CPP-MR. It also contains current in-plane CIP-MR data measured on samples prepared in the same sputtering system. Limited data and preliminary values of parameters from our CPP-MR studies were reported in Refs. 3–5.

We previously showed that a two-current, series-resistor (2CSR) model, valid for infinite spin-diffusion lengths, l_{sf} , in both the F and N layers of a multilayer, described well the CPP-MR's of Ag/Co (Refs. 6–10) and Cu/Co (Refs. 3, 8, and 10) multilayers with Ag or Cu layers thick enough that exchange coupling between the Co layers is negligible. The model allows the separation of the spin-dependent scattering contributions in the bulk F metal and at the F/N interfaces.^{7–10} These contributions are characterized by the spin-anisotropy parameters $\alpha_F=\rho_F^{\downarrow}/\rho_F^{\uparrow}$ and $\alpha_{F/N}=R_{F/N}^{\downarrow}/R_{F/N}^{\uparrow}$, where $\rho_F^{\uparrow(\downarrow)}$ and $R_{F/N}^{\uparrow(\downarrow)}$ are, respectively, the F -layer bulk resistivity and the interface resistance of electrons with spin parallel (antiparallel) to the F -layer magnetization M_i . The parameters β and γ used in the 2CSR model analysis are given by $\alpha_F=(1+\beta)/(1-\beta)$ and $\alpha_{F/N}=(1+\gamma)(1-\gamma)$. For both Ag/Co and Cu/Co, our derived CPP bulk parameter, $\alpha_{\text{Co}}\sim 3$ was noticeably smaller than the interface parameters, $\alpha_{\text{Co/Cu}}\sim 6$ (Ref. 8) and $\alpha_{\text{Co/Ag}}\sim 11$.⁹ For these multilayers, effects of interface scattering thus dominate the CPP-MR for Co layer thicknesses up to $t_{\text{Co}}\sim 40$ nm.

The analysis of Fert and Campbell¹¹ suggests that bulk spin-dependent scattering should be more important in Py than in Co. We thus chose Cu/Py as a system where we expected a larger α_F than those for Ag/Co and Cu/Co, although we recognized that correlations between bulk alloy parameters and those associated with MR's need not necessarily be strong.¹² From CIP-MR measurements, Dieny,¹³ Dieny *et al.*,¹⁴ and Gurney *et al.*¹⁵ concluded that spin-dependent scattering in Cu/Py occurs mostly in the bulk Py, with the former deriving $\alpha_{\text{Py}}\geq 8$. Parkin,¹⁶ in contrast, has argued that the Cu/Py CIP-MR is dominated by spin-dependent scattering at the interfaces. Lenczowski² derived values, $\alpha_{\text{Py}}=2.1\pm 0.3$ and $\alpha_{\text{Py/Cu}}=5.0\pm 0.4$. In the present paper, we estimate the CPP-MR values, $\alpha_{\text{Py}}=4.7_{-1.3}^{+2.3}$, and $\alpha_{\text{Py/Cu}}=7.3_{-2.4}^{+6}$.

This paper is organized as follows. In Sec. II we describe our samples and experimental techniques. In Sec. III, we

briefly describe the 2CSR model which assumes no spin flips either in bulk Cu or Py or at the Cu/Py interfaces, i.e., that both l_{sf}^N and $l_{sf}^F = \infty$. We then explain the need for the theory of Valet and Fert (VF),¹⁷ which goes beyond this approximation. In Sec. IV we compare CIP-MR and CPP-MR's for our sputtered Cu/Py multilayers. In Sec. V we explain how we approximate the AP states needed for analysis, and in Sec. VI we numerically fit the VF equations to the data to derive the parameters appropriate to our samples. In Sec. VII we test how well our parameters predict the specific resistances (AR=Area times resistance) of Co/Cu/Py/Cu multilayers without adjustment. In Sec. VIII, we summarize and conclude.

II. SAMPLES

Schematics of our CPP-MR samples can be seen elsewhere.^{5,9} The multilayer of interest is sandwiched⁹ between crossed Nb strips, which superconduct at our measuring temperature of 4.2 K, thereby ensuring a uniform current flow through the multilayer, of area $A \sim 1.25 \text{ mm}^2$, where the strips overlap. The potential across the sample [including the superconducting/ferromagnetic (S/F) contacts] is measured using a superconducting quantum interference device null detector.

All of the samples were sputtered onto Si(100) substrates⁹ at sputtering pressure $\sim 2.5 \text{ mTorr}$. The sputtering rates were $\sim 1.2 \text{ nm/s}$ for Cu, $\sim 0.8 \text{ nm/s}$ for Py, and $\sim 0.9 \text{ nm/s}$ for Nb. The substrate temperature was held between -40 and $+20 \text{ }^\circ\text{C}$. Both the CPP and CIP multilayers with $t_{\text{Py}} = 1.5 \text{ nm}$ were grown on 5 nm thick Py buffer layers sputtered onto the bare Si for the CIP samples and onto the Nb for the CPP samples. The other CPP multilayers were sputtered directly onto the Nb, starting with a Py layer. All of the CPP multilayers had the same total thickness, $t_T = 360 \text{ nm}$. The other CIP samples were sputtered with a 5 nm thick Py buffer onto 1.25 cm square substrates and then cleaved to produce narrower strips for MR and magnetization M measurements. Since the geometrical factor was not well defined for the CIP samples, only their MR's are given.

X-ray fluorescence studies of 300 nm thick films of sputtered Py and chips from a Py target showed that the target material had the expected composition of $\text{Ni}_{80}\text{Fe}_{20}$, but that the sputtered Py was about $\text{Ni}_{84}\text{Fe}_{16}$.

The intrinsic CPP quantity is the specific resistance AR.⁷ Figure 1 shows AR(H) and $M(H)$ for an exchange-decoupled Cu/Py sample. H_c is only a few Oe. $R(O)$ designates the resistance of the sample in its as-prepared state before H is applied. Increasing H from zero gradually reduces $R(H)$ until it reaches its minimum value, $R(S)$, above H_s . Thereafter, upon cycling from $+H_s$ to $-H_s$, $R(H)$ varies between $R(S)$ and a locally maximum value $R(Pk)$ that occurs at a field H_{Pk} near the coercive field H_c where $M=0$. In Ag/Co and Cu/Co, we have always found $R(O) \geq R(Pk)$.⁸ In Cu/Py, in contrast, this is not always so, and the difference will be important to our data analysis.

The analysis of Sec. VI below assumes advance knowledge of three parameters, the Cu and Py layer resistivities, ρ_{Cu} and ρ_{Py} , and twice the Nb/Py interface resistance, $2AR_{\text{Nb/Py}}$. $2AR_{\text{Nb/Py}}$ was estimated as the ordinate intercept

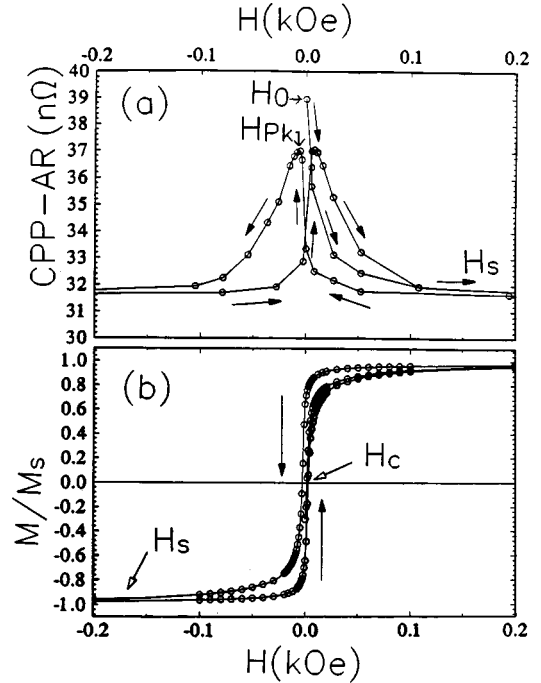


FIG. 1. (a) The CPP AR for a $[\text{Py}(6 \text{ nm})/\text{Cu}(8.4 \text{ nm})] \times 25$ sample. (b) The magnetization of the same sample.

of a linear plot of measured values of AR vs t_{Py} for sputtered sandwiches of Nb/Py/Nb with fixed $t_{\text{Nb}} = 300 \text{ nm}$. Rather scattered data gave $2AR_{\text{Nb/Py}} = 6.5 \pm 1.0 \text{ f}\Omega \text{ m}^2$ and (from the slope) $\rho_{\text{Py}} = 108 \pm 20 \text{ n}\Omega \text{ m}$.

Values for ρ_{Py} and ρ_{Cu} were estimated from measurements on independently sputtered thin films. For Cu, measurements on 300 nm thick films, gave a simple average of $\rho_{\text{Cu}} = 5 \pm 1 \text{ n}\Omega \text{ m}$, consistent with what we previously found for Co/Cu multilayers.^{3,8} For Py, measurements on films of different thicknesses prepared over two years from different targets ranged from a low of 102 nΩ m to a high of 177 nΩ m. These values are the same order of magnitude as the resistivity for bulk Py of $\sim 150 \text{ n}\Omega \text{ m}$,¹⁸ and the only value for sputtered films we have found, Dieny's¹³ ρ_{Py} also $\approx 150 \text{ n}\Omega \text{ m}$. We use a judiciously weighted average $\rho_{\text{Py}} = 122 \pm 20 \text{ n}\Omega \text{ m}$, which is consistent to within mutual uncertainties with the alternative estimate $108 \pm 20 \text{ n}\Omega \text{ m}$ noted above.

III. THEORETICAL BACKGROUND

At 4.2 K, where scattering by phonons and magnons should be negligible, the momentum transferring spin-flip scattering lengths in sputtered metals and alloys are expected to be much longer than the layer thicknesses of typical multilayers (see Appendix A of Ref. 17). The current-carrying electrons can then be divided into two spin-channels that do not intermix.¹⁹ In Ag, Cu, and Co there is now good evidence that the values of l_{sf} at 4.2 K are much longer than the typical layer thicknesses.²⁰ To obtain the CPP specific resistance, one then first simply adds the bulk and interface specific resistances within each channel in series and then adds the specific resistances of the two channels in parallel.^{10,19} This is the 2CSR model.

If the total thickness, $t_T = Nt_{\text{Cu}} + Nt_{\text{Py}}$, of the multilayer is held fixed, and either t_{Py} is fixed and t_{Cu} is varied, or else one

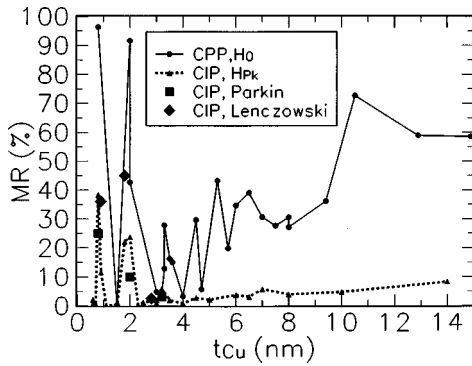


FIG. 2. Magnetoresistance as a function of copper thickness in the series $\text{Py}(5 \text{ nm})[\text{Py}(1.5 \text{ nm})/\text{Cu}(t_{\text{Cu}})] \times 14$. For comparison purposes all the CIP data are for H_{Pk} . Only the peak points of the Parkin (300 K) and Lenczowski (4.2 K) data are shown. Both our CIP and CPP data were taken at 4.2 K.

holds $t_{\text{Py}} = t_{\text{Cu}}$, then $\text{AR}(\text{AP})$ should vary linearly with N , the number of bilayers. The general expression for the P state is more complex, but except for very small N , $\text{AR}(\text{P})$ is also linear in N . Such linear variations, allow direct determinations of parameters from least-squares linear fits. The detailed equations on which our analysis of the Ag/Co and Cu/Co data was based can be found elsewhere.^{9,24}

When the present study began, we expected a long $l_{\text{sf}}^{\text{Py}}$, and hence the analyses in Refs. 3 and 4 used the simple 2CSR model. However, the recent results of Steenwyk *et al.*²¹ now suggest that $l_{\text{sf}}^{\text{Py}} \sim 5.5 \text{ nm}$. Handling a finite $l_{\text{sf}}^{\text{Py}}$ requires more complex equations derived by Valet and Fert (VF).¹⁷ Since $l_{\text{sf}}^{\text{Cu}}$ is still long, $l_{\text{sf}}^{\text{Py}}$ is the only additional parameter introduced in Eqs. (40)–(42) of Ref. 17. Our data analyses with finite $l_{\text{sf}}^{\text{Py}}$ must then be done numerically.

IV. COMPARISONS OF CIP- AND CPP-MR'S

Here, we compare our CPP-MR and CIP-MR data with each other and with the CIP-MR data of Parkin¹ and Lenczowski *et al.*² For this comparison, we subtract $2\text{AR}_{\text{Nb/Py}} = 6.5 \text{ f}\Omega \text{ m}^2$ from the denominators of the CPP-MR's to remove the contribution due to the Nb/Py interfaces.

Parkin found that the CIP-MR(Pk) of Cu/Py multilayers with fixed $t_{\text{Py}} = 1.5 \text{ nm}$, and measured at 300 K, oscillates in magnitude with increasing t_{Cu} .¹ Figure 2 shows our CIP-MR data for $\text{Py}(5 \text{ nm})[\text{Py}(1.5 \text{ nm})/\text{Cu}(t_{\text{Cu}})]_{14}$ taken at 4.2 K using, like Parkin and Lenczowski, the H_{Pk} data to approximate $R(\text{AP})$. The maxima data of Parkin (at 300 K) and Lenczowski (at 4.2 K) are included for comparison. For the CIP-MR, we found oscillations with essentially the same period as they did, and generally little difference between $R(O)$ and $R(Pk)$. Figure 2 shows that the CPP-MR is substantially larger than the CIP-MR. The larger magnitude of the CPP-MR data leads to the identification of at least 3 and possibly 5 maxima, corresponding to a mean period of 1.15 nm. The CPP-MR also retains its large value to much larger t_{Cu} than shown in Fig. 2 (e.g., it is still 45% for $t_{\text{Cu}} = 43.5 \text{ nm}$), whereas the CIP-MR tends rapidly to zero as t_{Cu} increases. These behaviors are expected for $l_{\text{sf}}^{\text{Cu}}$ long.¹⁹

Figure 1 also shows that for the particular sample illustrated, $R(O)$ was larger than $R(Pk)$, similar to the behavior

we found for most Cu/Co and Ag/Co multilayers. However, this was not always true for Cu/Py, as will be discussed in the next section.

V. ESTIMATING $\text{AR}(\text{AP})$

We now turn to the quantitative analysis of the CPP-AR's using the VF equations. As noted above, $\text{AR}(\text{P})$ is obtained simply by increasing the applied field H to above the saturation field H_s , where $R(H)$ reaches its minimum value $R(S)$. But estimating $\text{AR}(\text{AP})$ for samples with a wide range of values of t_{Cu} is not so simple.

At the first peak in Fig. 2, the antiferromagnetic exchange coupling is so strong that the measured AR should well approximate $\text{AR}(\text{AP})$. However, to achieve values of AR that vary monotonically with t_{Cu} and t_{Py} , as required by the VF equations, the samples that we analyze in this paper have large values of $t_{\text{Cu}} - t_{\text{Cu}} \geq 10 \text{ nm}$ —beyond the region where exchange coupling oscillating with t_{Cu} is appreciable. For large t_{Cu} , any coupling should be magnetostatic, and it is not obvious that this will produce AP ordering at low H . From theory, we expect the largest value of AR to best approximate $\text{AR}(\text{AP})$. As noted above, in Ag/Co and Cu/Co multilayers with $t_N \geq 6 \text{ nm}$, this was always $\text{AR}(O)$. $\text{AR}(O)$ was also larger than $\text{AR}(D)$, the value obtained after demagnetizing the sample by simultaneously reducing the magnitude of H while oscillating its sign.²² For Cu/Co, we have presented additional evidence that $\text{AR}(O)$ under such conditions is a good approximation to $\text{AR}(\text{AP})$.³

In Cu/Py, the situation is more complex. Figure 3 shows the ratios $R(O)/R(Pk)$ and $R(D)/R(Pk)$ for the three series of multilayers studied. [Note that these plots only contain results for samples for which $R(D)$ was measured.] In each case there were some samples in which $R(Pk)$ was greater than $R(O)$. However, with only two exceptions, $R(Pk)$ was less than $R(D)$. The best we can do is to approximate $R(\text{AP})$ by $R(L)$, the largest of $R(O)$ or $R(D)$. $R(L)$ is probably a lower bound on $R(\text{AP})$ for Cu/Py. In Sec. VII we will present evidence supporting the choice of $R(\text{AP}) \cong R(L)$.

VI. DATA, ANALYSIS, AND DISCUSSION

Figures 4–6, show the data for $\text{AR}(L) [\cong \text{AR}(\text{AP})]$ and $\text{AR}(\text{P})$ as a function of N for the three series, $t_{\text{Py}} = 1.5 \text{ nm}$, $t_{\text{Py}} = 6 \text{ nm}$, and $t_{\text{Py}} = t_{\text{Cu}}$. The solid lines are fits to the low- N data which we now describe.

In our earlier publication³ we only had $R(O)$ and $R(H_s)$ data for $t(\text{Py}) = 1.5$ and 6 nm . Using the 2CSR model, which assumes $l_{\text{sf}}^F = \infty$, values of β and γ were derived. Three occurrences since then necessitate a different analysis. First we have measured the $t_{\text{Py}} = t_{\text{Cu}}$ samples (which hereafter we call equals samples), and found that the above parameters failed to correctly predict their AR's. Second it is now clear that $R(L)$ should replace $R(O)$ in our analysis. Third, the recent work of Steenwyk *et al.*²¹ strongly suggests that $l_{\text{sf}}^{\text{Py}}$ is $\sim 5.5 \text{ nm}$. Such a short $l_{\text{sf}}^{\text{Py}}$ requires using the VF analysis of the $t_{\text{Py}} = 6 \text{ nm}$ and the equals data. Our present analyses are therefore based on taking $R(L) \sim R(\text{AP})$ and using the Valet-Fert equations, which apply when $l_{\text{sf}}^{\text{Py}}$ is finite.

It turns out that these modifications are insufficient to explain the $R(L)$ data for the equals series, which leads one to

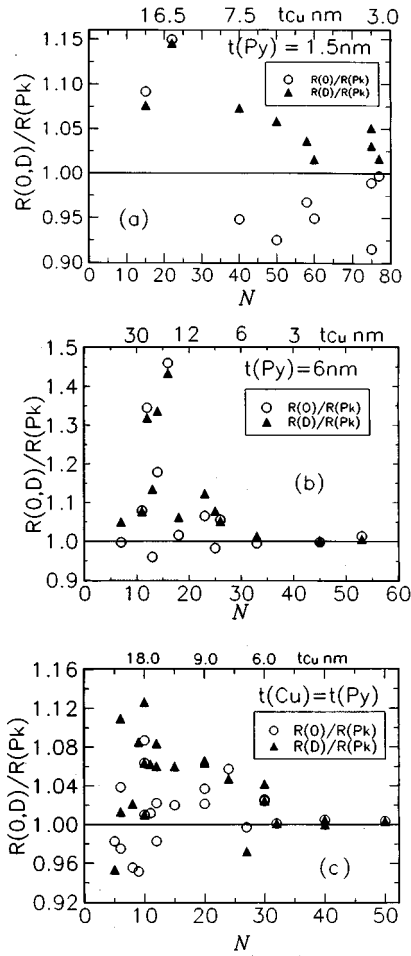


FIG. 3. The ratios $R(O)/R(Pk)$ and $R(D)/R(Pk)$ for (a) $t(Py)=1.5$ nm; (b) $t(Py)=6$ nm, and (c) $t(Py)=t(Cu)$. Points on the same vertical line are from the same sample. The migration of the empty circles to the full triangles after demagnetization indicates that R usually increased after demagnetization, and, with only two exceptions, $R(D)$ was $>R(Pk)$.

suspect these data do not approximate $R(AP)$. Further reason for this suspicion comes from the near coincidence of L and P data in Fig. 6 and from magnetization measurements, which show that the coercive field, H_c for equals samples is very small, e.g., only ~ 1.7 Oe for a $[Py(30 \text{ nm})/Cu(30 \text{ nm})] \times 6$ sample. We do not have magnetization data for all the samples, but the magnitude of H_{Pk} , which is usually

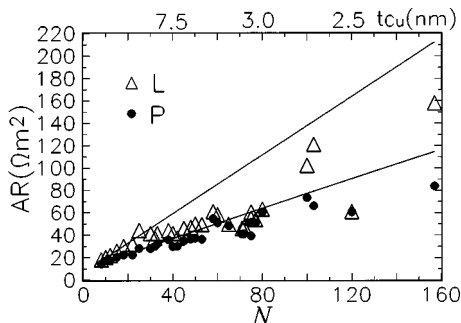


FIG. 4. $AR(L)$ and $AR(P)$ as a function of N for $t_{Py}=1.5$ nm. The lines are fits assuming $l_{sf}=5.5$ nm and using parameters in column 3 of Table I derived from the low N linear regions.

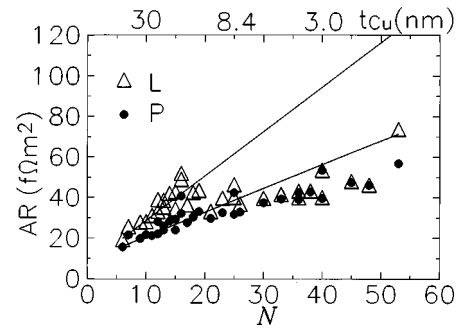


FIG. 5. As for Fig. 4, but for $t_{Py}=6$ nm.

$\sim H_c$, gives an indication of how H_c changes with t_{Py} . We find $H_{Pk} \sim 20, 7$, and 3 Oe for $t_{Py}=1.5$ nm, 6 nm, and the equals samples, respectively. Comparing these values with fields as large as 3 Oe at the sample due to the proximity of the sputtering gun, it is clear that the equal samples are grown in a field which is $\sim H_c$. We therefore omit the equals $AR(L)$ data from our main analysis given below.

The VF theory for $R(AP)$ requires the data to be closely linear in N . As was true for Cu/Co and Ag/Co , we must thus limit our analysis to values of N that satisfy this condition (i.e., to values of t_{Cu} large enough that the samples are not exchanged coupled). From Figs. 4 and 5, this limits the analysis for $t_{Py}=1.5$ nm to $N \leq 30$ and for $t_{Py}=6$ nm to $N \leq 16$. For the equals samples we take $N \leq 12$, which corresponds roughly with the minimum t_{Cu} thickness of the other samples.

In our analysis we assume initial values of $2AR_{Nb/Py} = 6.5 \text{ f}\Omega \text{ m}^2$, $\rho_{Cu}=4.5 \text{ n}\Omega \text{ m}$, $\rho_{Py}=122 \text{ n}\Omega \text{ m}$ and $l_{sf}^{Py}=5.5 \text{ nm}$. The fits were made by assuming values for the unknown parameters β and γ , calculating values of χ_i^2 for each β, γ pair, and for each of the $i=5$ sets of $AR(L)$ and $AR(P)$ data used, and choosing as the best parameters those that minimize the overall $\sum_i \chi_i^2$.

The fits are shown as solid lines in Figs. 7–9, and the parameters are given in column 3, Table I. We take $\beta=0.65$ and $\gamma=0.76$ as our best estimates. To obtain some estimate of the uncertainty in these values we have performed two other analyses which we take as extreme cases. In the first we fit the same data but assumed $l_{sf}^{Py}=500 \text{ nm}$ —effectively the infinite value corresponding to the 2CSR model. These fits are shown as dotted lines in Figs. 7–9, and the corresponding parameters are listed in column 1, Table I. In the second we used all the data [including the previously omitted $R(L)$ data for the equals samples] but left l_{sf}^{Py} and ρ_{Py} free, to

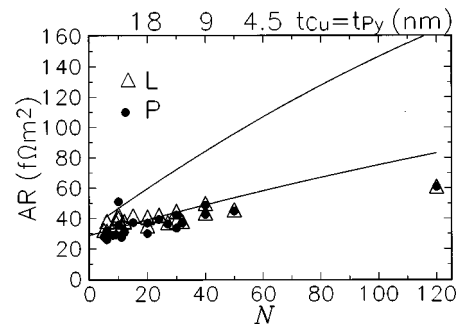


FIG. 6. As for Fig. 4, but for $t_{Py}=t_{Cu}$.

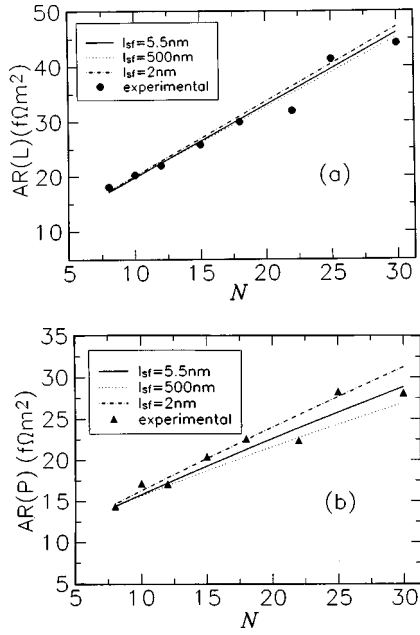


FIG. 7. (a) $AR(L)$ and (b) $AR(P)$ for the $t_{Py} = 1.5$ nm data plotted as a function of N for the three analyses outlined in the text. Only the data in the linear range are included.

see if we could account for the equals $AR(L)$ data in this way. These fits are shown as dash/dot lines in Figs. 7–9, and the parameters are listed in column 2, Table I. The equals $AR(L)$ fit is indeed improved, but only at the expense of worsened fits to the other data, plus l_{sf}^{Py} and ρ_{Py} values which are outside the range of likelihood. Comparing the values of β and γ for the three different columns in Table I reveals that the variation is not very large. Having taken the

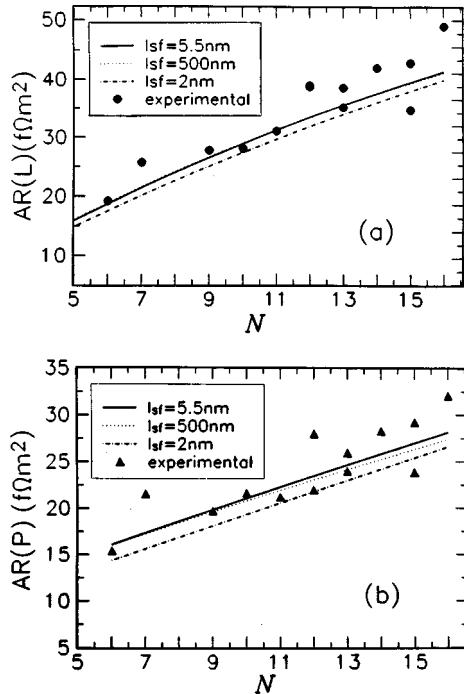


FIG. 8. As for Fig. 7, but $t_{Py} = 6$ nm. In (a) data for $l_{sf} = 55$ and 500 nm are scarcely distinguishable.

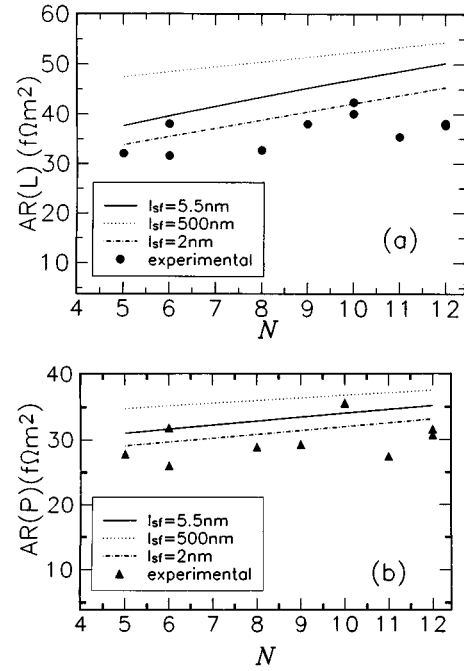


FIG. 9. As for Fig. 7 but $t_{Cu} = t_{Py}$.

parameters for $l_{sf}^{Py} = 5.5$ nm as our preferred ones, it seems conservative to take those for $l_{sf}^{Py} = 500$ nm and 2 nm as extremes. We thus estimate $\beta = 0.65 \pm 0.1$ and $\gamma = 0.76 \pm 0.1$.

To check the reliability of these parameters we turn to a completely independent set of experiments on Co/Cu/Py/Cu hybrid multilayers.^{5,23,24} We ask how well these parameters for Py allow us to predict the values of $A\Delta R$ for these hybrids with no adjustability. Success in such a prediction will support our values of β and γ .

VII. PREDICTIONS FOR Co/Cu/Py/Cu HYBRIDS

When the Cu layers in these hybrids are thick enough to uncouple the exchange interaction between Co and Py layers, the very different saturation fields of sputtered thin layers of Co ($H_s^{Co} \sim 200$ Oe) and Py ($H_s^{Py} \sim 10$ Oe) lead naturally to an AP state. If a field $> +H_s^{Co}$ is first applied and then reduced to just beyond $-H_s^{Py}$, the magnetizations of the Co layers will still be aligned along the initial field direction, but those

TABLE I. Parameters from the fit of the data to the Valet-Fert (Ref. 17) equations assuming three different values of l_{sf}^{Py} . ρ_{Py} was fixed in columns 1 and 3. Values in rows 2–5 were obtained through the minimalization of $\Sigma \chi^2$ as described in the text. Our best values of β , γ , α_{Py} , and $\alpha_{Cu/Py}$ appear in column 3.

	$l_{sf}^{Py} = 500$ nm	$l_{sf}^{Py} = 2$ nm	$l_{sf}^{Py} = 5.5$ nm
ρ_{Py} (nΩ m)	122	110	122 ± 20
ρ_{Cu} (nΩ m)	5	4.5	5
$2AR_{Nb/Py}$ (fΩ m ²)	6.5	6.1	6.1
β	0.63	0.77	0.65 ± 0.1
γ	0.82	0.66	0.76 ± 0.1
α_{Py}	4.4	7.7	$4.7_{-1}^{+2.3}$
$\alpha_{Cu/Py}$	10	4.9	$7.3_{-2.4}^{+6}$

of the Py layers will be reversed, producing an antiparallel alignment of the Co and Py magnetizations. The corresponding measured $R(AP)$ does *not* depend on the Cu/Py multilayer assumption that $R(AP) = R(L)$.

The raw data for $AR(AP)$ of the hybrid samples appears in the paper by Pratt *et al.*²⁴ Because $A\Delta R$ is more sensitive than $AR(AP)$ and $A(P)$, in Fig. 10 we choose to show data for $A\Delta R$ for $[Cu/Py/Cu/Co] \times N$ samples with $t_{Cu} = 20$ nm, $t_{Co} = 6$ nm, and $t_{Py} = 10$ or 16 nm. We include two theoretical calculations: The lower curve is a previously published one,²⁴ using older parameters based on less data and assuming $R(AP) \cong R(O)$, and $l_{sf}^{Py} = \infty$. The upper curve uses the present parameters for $l_{sf}^{Py} = 5.5$ nm. Even better fits using the present parameters are obtained to the experimental hybrid data (published as $A\Delta R$ in Ref. 25) on samples with $t_{Cu} = 20$ nm, $t_{Co} = 3$ nm, and $t_{Py} = 5$ or 8 nm. In all of the hybrid samples, the fits to the data using the present parameters are superior to those using the older parameters. This strongly supports the approximation $R(L) \cong R(AP)$ for Cu/Py. We emphasize that the prediction of the $[Co/Cu/Py/Cu] \times N$ data represents a completely independent test of our new parameters, because the hybrid data were not used in deriving the new parameters.

We conclude this section by noting that Hsu *et al.*²⁶ estimated possible effects on β and γ of spin-flip scattering at the Cu/Py interface due to alloying of Cu and Ni (since Fe is the minority constituent of Py). They concluded that any such scattering would increase β and γ by no more than a few percent, well within our specified uncertainties. While their analysis assumed that $l_{sf}^{Py} = \infty$, a shorter l_{sf}^{Py} should not significantly change their conclusion.

VIII. SUMMARY AND CONCLUSIONS

We have presented data on the CPP-MR and CIP-MR for three different series of Cu/Py multilayers: fixed $t_{Py} = 1.5$ nm; fixed $t_{Py} = 6$ nm; and $t_{Py} = t_{Cu}$. For fixed $t_{Py} = 1.5$ nm, both our CIP-MR and CPP-MR data show oscillations with increasing t_{Cu} with the same period as that previously reported by Parkin.¹ In all three cases, we find the CPP-MR to be several times larger than the CIP-MR. We have used the Valet-Fert¹⁷ theory to analyze the CPP-MR data for samples with t_{Cu} thick enough to make exchange coupling small. Our resulting best estimates for the appropriate parameters are given in column 3 of Table I. The main conclusion is that β and γ are similar in size. This similarity indicates that, at least in the CPP-MR, spin-dependent scattering in the bulk Py and at Cu/Py interfaces are both important. Our best value of $\alpha_{Py} \sim 4.7^{+2.3}_{-1.3}$ falls between the values $\alpha_{Py} \geq 8$ (Ref. 13)

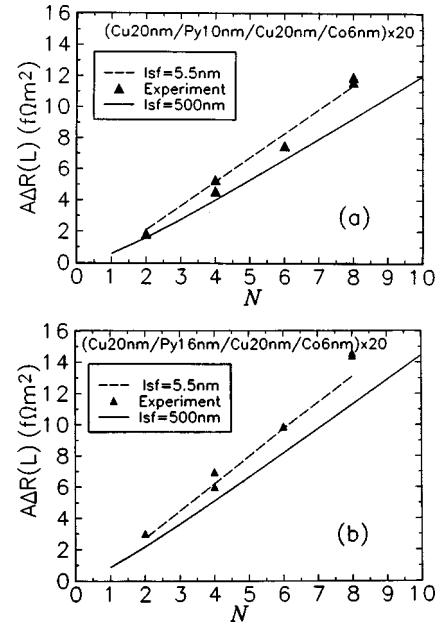


FIG. 10. Predictions for the hybrid sample (a) $[Cu(20 \text{ nm})/Py(10 \text{ nm})/Cu(20 \text{ nm})/Co(6 \text{ nm})] \times 20$. (b) $[Cu(20 \text{ nm})/Py(16 \text{ nm})/Cu(20 \text{ nm})/Co(6 \text{ nm})] \times 20$.

and $\alpha_{Py} \sim 2.1$ (Ref. 2) estimated from CIP measurements. Our upper bound just overlaps the range of $\alpha \sim 7-20$ reported by Campbell and Fert^{11,27} for Fe in *bulk dilute NiFe* alloys.

We have explained carefully the assumptions and uncertainties underlying our analysis. Because of those assumptions, and the uncertainty in establishing $AR(AP)$, we have chosen to specify relatively large systematic uncertainties in the parameters β_{Py} and $\gamma_{Py/Cu}$. We also cannot say how applicable these parameters might be to Cu/Py multilayers prepared under very different conditions or in different ways. We note, however, that our latest parameters do well in fitting independent data for sputtered Co/Cu/Py/Cu multilayers where the AP and P states are both well defined.

Finally much of the uncertainty in this work apparently arises from the very small coercive field of Permalloy and the effects of the magnetic field of the sputtering guns. We hope that our experience will warn other workers of this problem.

ACKNOWLEDGMENTS

This work was supported in part by the Ford Scientific Laboratory, by the NSF under Grants No. MRSEC-94-004127, DMR-94-23795, and by the Michigan State University Center for Fundamental Materials Research.

*Present address: Center for Condensed Matter Sciences, National Taiwan University, 1 Roosevelt Road, Sec. 4, Taipei, Taiwan 106.

¹S. S. P. Parkin, *Appl. Phys. Lett.* **60**, 512 (1992).

²S. K. J. Lenczowski, M. A. M. Gijs, R. J. M. Van de Veerdonk, J. B. Giebers, and W. J. M. De Jonge, in *Magnetic Ultrathin Films, Multilayers and Surfaces*, edited by A. Fert *et al.*, MRS Symposium Proceedings No. 384 (Materials Research Society, Pittsburgh, 1995), p. 341.

³P. A. Schroeder, J. Bass, P. Holody, S.-F. Lee, R. Loloee, W. P. Pratt, Jr., and Q. Yang, in *Magnetic Ultrathin Films, Multilayers*

and Surfaces/Interfaces, edited by B. T. Jonker *et al.*, MRS Symposium Proceedings No. 313 (Materials Research Society, Pittsburgh, 1993), p. 47.

⁴J. Bass, P. A. Schroeder, W. P. Pratt, Jr., S. F. Lee, Q. Yang, P. Holody, L. L. Henry, and R. Loloee, *Mater. Sci. Eng., B* **31**, 77 (1995).

⁵Q. Yang, P. Holody, R. Loloee, L. L. Henry, W. P. Pratt, Jr., P. A. Schroeder, and J. Bass, *Phys. Rev. B* **51**, 3226 (1995).

⁶S. F. Lee, W. P. Pratt, Jr., R. Loloee, P. A. Schroeder, and J. Bass, *Phys. Rev. B* **46**, 548 (1992).

- ⁷S. F. Lee, W. P. Pratt, Jr., Q. Yang, P. Holody, R. Loloee, P. A. Schroeder, and J. Bass, *J. Magn. Magn. Mater.* **118**, 1 (1993).
- ⁸P. A. Schroeder, J. Bass, P. Holody, S. F. Lee, R. Loloee, W. P. Pratt, Jr., and Q. Yang, in *Magnetism and Structure in Systems of Reduced Dimension*, NATO ASI Series B Vol. 309, edited by R. F. C. Farrow *et al.* (Plenum, New York, 1993), p. 129.
- ⁹S.-F. Lee, Q. Yang, P. Holody, R. Loloee, J. H. Hetherington, S. Mahmoud, B. Ikegami, K. Vigen, L. L. Henry, P. A. Schroeder, W. P. Pratt, Jr., and J. Bass, *Phys. Rev. B* **52**, 15 426 (1995).
- ¹⁰W. P. Pratt, Jr., S.-F. Lee, P. Holody, Q. Yang, R. Loloee, J. Bass, and P. A. Schroeder, *J. Magn. Magn. Mater.* **126**, 406 (1993).
- ¹¹A. Fert and I. A. Campbell, *J. Phys. F* **6**, 849 (1976).
- ¹²P. M. Levy, in *Solid State Physics Series*, edited by H. Ehrenreich and D. Turnbull (Academic, New York, 1994), Vol. 47, p. 374.
- ¹³B. Dieny, *Europhys. Lett.* **17**, 261 (1992); *J. Phys.: Condens. Matter* **4**, 8009 (1992).
- ¹⁴B. Dieny, V. S. Speriosu, J. P. Nozieres, B. A. Gurney, A. Vedyayev, and N. Ryzhanova, in *Magnetism and Structure in Systems of Reduced Dimension* (Ref. 8), p. 279.
- ¹⁵B. A. Gurney, V. S. Speriosu, J.-P. Nozieres, H. Lefakis, D. R. Wilhoit, and O. U. Need, *Phys. Rev. Lett.* **71**, 4023 (1993).
- ¹⁶S. S. P. Parkin, *Appl. Phys. Lett.* **61**, 1358 (1992).
- ¹⁷T. Valet and A. Fert, *Phys. Rev. B* **48**, 7099 (1993).
- ¹⁸See, for example, D. Jiles, *Introduction to Magnetism and Magnetic Materials* (Chapman and Hall, New York, 1991), p. 281.
- ¹⁹S. Zhang and P. M. Levy, *J. Appl. Phys.* **69**, 4786 (1991).
- ²⁰Q. Yang, P. Holody, S.-F. Lee, L. L. Henry, R. Loloee, P. A. Schroeder, W. P. Pratt, Jr., and J. Bass, *Phys. Rev. Lett.* **72**, 3274 (1994).
- ²¹S. D. Steenwyk, S. Y. Hsu, R. Loloee, J. Bass, and W. P. Pratt, Jr., *J. Magn. Magn. Mater.* **170**, L1 (1997).
- ²²P. A. Schroeder, S.-F. Lee, P. Holody, R. Loloee, Q. Yang, W. P. Pratt, Jr., and J. Bass, *J. Appl. Phys.* **76**, 6610 (1994).
- ²³J. Bass, P. A. Schroeder, W. P. Pratt, Jr., S.-F. Lee, Q. Yang, P. Holody, L. L. Henry, and R. Loloee, *Mater. Sci. Eng., B* **31**, 77 (1995).
- ²⁴W. P. Pratt, Jr., Q. Yang, L. L. Henry, P. Holody, W.-C. Chiang, P. A. Schroeder, and J. Bass, *J. Appl. Phys.* **79**, 5811 (1996).
- ²⁵W. P. Pratt, Jr., S. D. Steenwyk, S. Y. Hsu, W.-C. Chiang, A. C. Schaefer, R. Loloee, and J. Bass, *IEEE Trans. Magn.* **33**, 3305 (1997).
- ²⁶S. Y. Hsu, P. Holody, R. Loloee, J. M. Rittner, W. P. Pratt, Jr., and P. A. Schroeder, *Phys. Rev. B* **54**, 9027 (1996).
- ²⁷I. A. Campbell and A. Fert, in *Ferromagnetic Materials*, edited by E. P. Wohlfarth (North-Holland, Amsterdam, 1982), Vol. 3, Chap. 9.